Algorithmic optimisation of the electrical power output of a low-cost, multicore thermoacoustic engine with varying resonator pressure

F. Huntingford[1*], **W. Kisha**[1]

[1]Faculty of Engineering, University of Nottingham, UK, NG7 2RD
[*]Corresponding author: franhunts@outlook.com

Abstract

Incorporating thermoacoustic engines (TAEs) into clean cooking stoves offers to reduce rural energy poverty while cutting morbidity associated with smoke inhalation. TAEs are used to generate electricity from the waste heat of a cooking fire to provide power for lighting and personal devices. This study investigated the effect of TAE mean pressure using a numerical model of a twin-core, asymmetrically heated TAE. Automation code was developed to allow the numerical model to be optimised using the Nelder-Mead algorithm to maximise electrical power output at each mean pressure. The parameters available for optimisation were the length and position of two side volumes (stubs). A maximum electrical output of 59.63 W was determined at 2.2 bar mean pressure. This is a 90% increase on the original numerical model at atmospheric pressure. Simulation-based optimisation, as performed in this study, is identified as being universally applicable to the design of TAEs.

Keywords: thermoacoustic, DeltaEC, simulation-based optimisation

1. Introduction

The 7th United Nation's Sustainable Development Goal is to "Ensure access to affordable, reliable, sustainable and modern energy for all" [1]. Despite significant advancements in energy technologies, progress is rapidly required if this global energy target is to be met by 2030. Cooking and electricity generation in rural areas are two sectors that require particular attention in developing countries.

In 2016, some 2.8 billion people used polluting open fires or simple, solid-fuel stoves to cook [2]. This statistic has a significant overlap with the 13% of the global population who have no access to electricity [1]. When solid fuels combust, they emit gaseous and particulate pollutants which were attributable to 1.8 million deaths in 2017 [3].

The SCORE (Stove for Cooking, Refrigeration and Electricity) project (www.score.uk.com) is an initiative established in 2007 to incorporate electricity generation into efficient cooking stoves. Adding this secondary function to clean cooking stoves has the potential to increase their uptake, as the device is more attractive to the entire household. Small scale, domestic electricity production enables the powering of lighting and personal electronics. Furthermore, the efficient use of resources for multiple purposes has the potential to reduce fossil fuel use and decrease greenhouse gas emissions.

The stove under development uses a travelling-wave thermoacoustic engine (TAE) to convert waste heat from solid fuel combustion into electricity. This technology has been identified as a potential low cost, low maintenance alternative to more mature electricity generating techniques [4]. Both these advantages are due to the fact that these engines have very few moving parts. Riley [4] concluded that thermoacoustic electricity generation incorporated into a stove is more cost-effective than community-sized solar and wind technologies, but more expensive than hydropower. However, hydropower installation is limited by local geography.

Prototypes have been produced by the SCORE program, but to date they fall short of the design target of 100 W of electricity generation. Multi-core TAEs are being considered to address this shortfall [5]. Despite higher complexity, they have been shown to have a lower onset temperature [6] and increased power output [7].

2. Background

2.1 Thermoacoustic Engines

Thermoacoustic engines take advantage of the repeated adiabatic compression and expansion of a gas through which acoustic waves are travelling [8]. A thermodynamic cycle is achieved by controlling heat input to the oscillating fluid. This thermodynamic cycle acts to strengthen an existing acoustic wave, thereby developing acoustic power. The heat exchange from the heat source into the working fluid occurs in the combination of components known as the core. The developed acoustic power can then be converted to an electrical output using a transducer such as a linear alternator [9] or bidirectional turbine [10]. However, commercially available loud-speakers (operated in reverse) are often used as a substitute to purpose-designed linear alternators due to their acceptable power conversion efficiency and low cost [11]. The transducer is placed in series with the oscillating fluid causing the movement of a mechanical component, from which electricity is generated using the motor effect.

Thermoacoustic engines are broadly categorised by the predominant characteristic of the acoustic wave (standing or travelling wave) as it undergoes a thermodynamic cycle in the core. Acoustic waves within a TAE consist of varying proportions of standing and travelling waves. The standing waves occur as a result of reflection and subsequent interference of travelling waves.

Travelling wave engines are often configured with a looped feedback pipe. In this configuration of TAE, heat exchange between the gas and the solid occurs in the regenerator. A thermal gradient is established across the regenerator through the use of heat exchangers. Gas is able to oscillate in this area while maintaining high thermal contact with the solid medium. Figure 1 shows a diagram of a typical travelling wave TAE. The details of the thermodynamic cycle in this type of TAE are described by Swift [12].

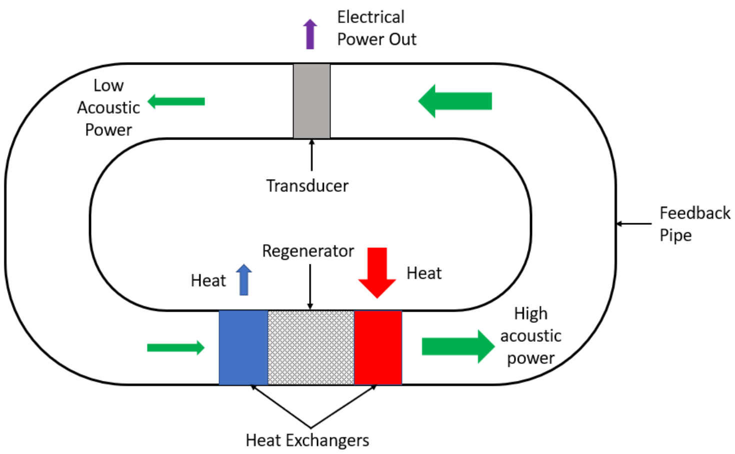

Figure 1. A representation of a single core, travelling wave TAE.

Thermoacoustic engines present difficulties to designers due to complicated system-level effects. Individual variable effects are poorly understood, and a substantial proportion of design variables are confounded. An approach to improving performance, considering system-level effects only, without comprehensive understanding of individual parameters is applicable given the current state of knowledge.

2.2 Selected opportunities for performance increase

Thermoacoustic theory indicates that increasing the mean pressure in a given thermoacoustic system will also increase acoustic power. This is indicated by the dimensionless group [13] :

$$\frac{\dot{E}}{p_m A a} \tag{1}$$

Where $\dot{E}$ is the acoustic power, p_m is mean pressure, A the cross sectional-area of the regenerator and a the speed of sound.

Pressurisation to the order of 100 bar is used in some applications [14], however, high pressurisation is not an option for a low-cost TAE due to the cost of manufacture. The investigation of electrical power output at slightly elevated pressure will determine economic feasibility, considering the manufacturing cost penalty. Pressurisation to moderate pressure (5 bar) is possible using a bicycle pump.

Chen, et al. [5] found that by increasing the mean pressure of a TAE from atmospheric to 1.51 bar resulted in a 45% increase in power output. Their simulations showed that an increase to 2.1 bar would further increase performance but they were limited by the structural integrity of the prototype to experimentally validate this. Riley [11] experimented with increasing pressure in a demonstration TAE which found a peak in developed electrical output at 2 bar.

Mean pressure is a confounded variable with many acoustic parameters of a TAE [12]. The position and length of two side-volumes (stubs) located on the TAE loop also influence the acoustic field and can be adjusted to maximise performance [15]. These parameters can be tuned to maximise electrical output for each mean pressure.

The process of tuning the stub parameters to manipulate the acoustic field has been approached in several ways. Abdoulla-Latiwish and Jaworski [16] increased and decreased the dimensions of each component individually until a maximum output was found. Yu, et al. [17] selected the position for their stub experimentally, acknowledging there was room for improvement. They found that introducing a tuning stub to their prototype increased electrical output by 10-15% and reduced onset temperature by 40-50°C.

The tuning process is ideally repeated after each major design revision of a TAE, and therefore methods to streamline this process are desirable. Currently this is a time-consuming process involving manual manipulation of the design parameters in simulation software.

2.3 Simulation-based Optimisation

Applying an automated approach to supplement the design process can free up the time of a skilled researcher by allowing tedious tasks to be undertaken computationally. Automated control of the simulation software will allow for the use of optimisation algorithms, resulting in a faster process and higher confidence in an optimal configuration. The field of simulation-based optimisation has advanced in recent years to become widespread with regards to computational fluid dynamics and finite element analysis [18].

Automation also allows for fast sampling of a design with changing parameters, allowing for detailed insights into parameter interactions. Using automated data gathering is likely to encourage a structured approach to design, thereby enabling data driven conclusions. For example, a human may choose a parametric design approach for practicality, however this is still time consuming and leads to partial optimisation. A balance must be struck such that time is not wasted developing an automation technique, when a manual approach is sufficient.

Automation may be particularly applicable to research where it is wished to study the changing effect of one parameter. The confounded nature of TAE variables may require that a particular TAE is 'tuned' for each level of the investigated parameter. Automation is a fast and low-labour method of achieving this many hundreds of times. For example, this tuning may involve modifying the feedback tube length or the position and length of tuning stubs.

Design of Experiments (DOE) is an established tool for maximising the amount of information gained from a study while minimizing required data collection [19]. DOE specifies that parameters are varied simultaneously, and the response measured allowing convenient identification of parameter effects and relationships. These relationships can be used to determine a globally optimum design. A DOE approach is excellent for establishing relationships over a small input space but suffers limitations when the scale and dimensionality of the input space increase due to the number of sample points required.

Global optimisation algorithms can be applied directly to a TAE simulation. These algorithms sample the simulated model with varying parameters in order to determine an optimum design within the defined parameter boundaries. Common global optimisation techniques applied to simulation-based optimisation are Response Surface Methodology, Metaheuristics and Stochastic optimisation.

A local search is an alternative to finding a global optimal solution, at the sacrifice of the information and insights gained from a global search. Local search algorithms incrementally change parameters in the hope of improving the solution until some criteria is met, such as time elapsed or convergence. However, little to no information on parameter effects is gained and the solution may converge to a local optimum.

The Nelder-Mead method [20] is a popular numerical method for simulation-based optimisation. Various modifications and hybridisations are used for component design e.g. topology optimisation [21]; and system design e.g. nuclear reactor core design [22] and low energy building design [23]. This method is well suited to working with expensive-to-evaluate, 'black-box' functions due to the minimal number of function evaluations needed and the fact that no gradient information of the objective function is required [24]. The Nelder-Mead method is considered heuristic due to the problem of explicitly proving convergence of an optimal solution [25].

3. Methodology

This paper investigates the relationship between electrical power output and mean operating pressure. The results are obtained by simulation. A methodology was developed which required simulating the TAE in software, developing an automated sampling approach to the simulation, and then deciding upon and implementing an optimisation approach.

3.1 DeltaEC Model

The behaviour of TAEs is complicated to model analytically due to interacting acoustic and thermal physics. It is therefore required to numerically simulate the engine behaviour. DeltaEC [26] is a program used by researchers to design and evaluate the performance of thermoacoustic devices. DeltaEC is based on linear thermoacoustic theory. Thermoacoustic parameters are calculated within a user-defined geometry via numerical integration of continuity, energy and momentum equations in one spatial dimension. Time dependence is sinusoidal. A guess-target shooting method is used to satisfy the user defined boundary conditions. Therefore, the guesses for each run must be sufficiently accurate or the simulation will not converge. A success or fail indication is given at the end of each run indicating simulation convergence.

The TAE under investigation by this paper is the asymmetrically heated, twin-core SCORE stove prototype, pictured in Figure 2a). A model of this TAE has been developed and validated in DeltaEC by Kisha, et al. [27], of which the layout is shown in Figure 2b). The majority of the dimensions of the system are defined by either previous design processes or premanufactured parts and can be found in a thesis by Chen, et al. [5]. The engine receives 2.5 kW of heat input, with 40% of the heat applied to core 1 and 60% of the heat applied to core 2. The current model outputs 31.4 W of electrical power [27].

a)

b)

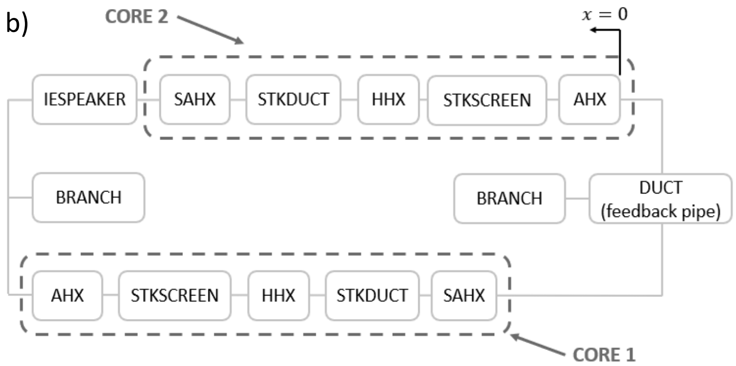

Key

HX (the ambient, secondary ambient, and hot heat exchangers); STKSCREEN (regenerator); STKDUCT (thermal buffer tube); IESPEAKER (linear alternator); BRANCH (tuning stub) and DUCT (used as a waveguide between all components – only included in the figure for the feedback pipe).

Figure 2. a) Twin core TAE prototype [28] b) Schematic of the twin core TAE.

The boundary conditions for the DeltaEC model are:

- Pressure magnitude and phase are matched at the start and end of the loop.
- Volumetric velocity magnitude and phase are matched at the start and end of the loop.

- The temperature after the thermal buffer tube is ambient.
- The phase of the electrical impedance of the alternator is forced to 180° i.e., purely resistive.

3.2 Optimisation Constraints

Design freedom to improve the DeltaEC model was given to five parameters: the position and length of two stubs (BRANCH in Figure 2b) as well as the mean pressure. The length of each stub is initially considered in terms of the imaginary component of its acoustic impedance, $Im(Z)$, as this is the quantity defined in DeltaEC. An approximation of equivalent length is then determined using the equations detailed by Yu, et al. [29]:

$$\frac{1}{3}\rho_M\omega^2 l^2 - A_{stub}\omega Im(Z)l - \rho_M a^2 = 0 \tag{2}$$

Where ρ_M is the mean density of the working gas; ω is the angular frequency of the acoustic wave in the engine; A_{stub} is the cross-sectional area of the tuning stub; l is the length of the stub; $Im(Z)$ is the imaginary part of the impedance of the stub; and a is the speed of sound. All of these values are available from the DeltaEC model.

The parameters were bounded as shown in Table 1 where the position (x) is consistent with Figure 2b.

Parameter	Lower Bound	Upper Bound	Reasoning
Im(Z) Stub 1	-3.5 MPa.s/m^3	-0.5 MPa.s/m^3	Estimated from experience of corresponding stub length
Im(Z) Stub 2	-3.5 MPa.s/m^3	-0.5 MPa.s/m^3	
Stub 1 Position (x)	0.924 m	4.124 m	Position of speaker and Core 1
Stub 2 Position (x)	0.267 m	0.817 m	Position of Core 1 and Core 2
Mean Pressure	Atmospheric	5 bar	Max pressure achievable with bicycle pump

Table 1. Parameters with design freedom and their associated bounds.

In this study, TAE performance is defined by the electrical power output from the loudspeaker (IESPEAKER in Figure 2b). Electrical power developed by the loudspeaker is influenced by the electrical load resistance. Finding the load resistance that maximises electrical power output is known as load matching. Load matching is applied in this study when comparison between sample points is required.

3.3 Automated Sampling of DeltaEC

Automated sampling of the simulation software is required before optimisation algorithms can be implemented. A routine was developed such that a control script could request an evaluation of a DeltaEC model with a particular set of parameters. The script then returns the resulting performance parameter, which in this case is the electrical power output.

Automation of DeltaEC is achieved using the set of python modules ‘pywinauto’, that enable automation of the Windows graphical user interface. An application programming interface (API) or other data transfer tool would be a faster way of automating DeltaEC, but this is not currently supported. Python was chosen as the language for automation due to the availability of a large library of useful modules, and the ease of learning for a beginner. In all cases the automation was performed on an Intel i7 processor at 1.8 GHz.

Sampling of a DeltaEC model requires a tailored approach due to the obligation of slowly incrementing parameters from one sample point to the next [26], in order to keep the guesses sufficiently accurate for the simulation to converge. Every model/sample point is generated via iteration from an existing model. This fact is further argument for developing an automated approach. DeltaEC uses a guess-target shooting routine for each run with the guesses updated from the results of the previous run. Incrementing the parameters by small amounts ensures the guesses are suitably accurate. This 'travel' between sample points is a chokepoint in the automation code because inputting new parameters and running DeltaEC is relatively slow. Faster sampling of the model was achieved by saving successful models and keeping a log. The log is then consulted after choosing a new sampling point, in order to select the model with parameters closest to the desired sampling point. The parameters in the log are scaled to account for differing units, and the Chebyshev distance between scaled parameters is used to define 'closeness'. The Chebyshev distance is the greatest of the differences along each dimension. This metric is also used to calculate the number of increments required for a particular travel between sample points. For the case when multiple sample points are known in advance, the sample points are ordered by solving the travelling salesman problem with Chebyshev distance in order to minimise travel distance and therefore minimise the time taken for automation. The process of sampling DeltaEC for a single sample point is shown in Figure 3.

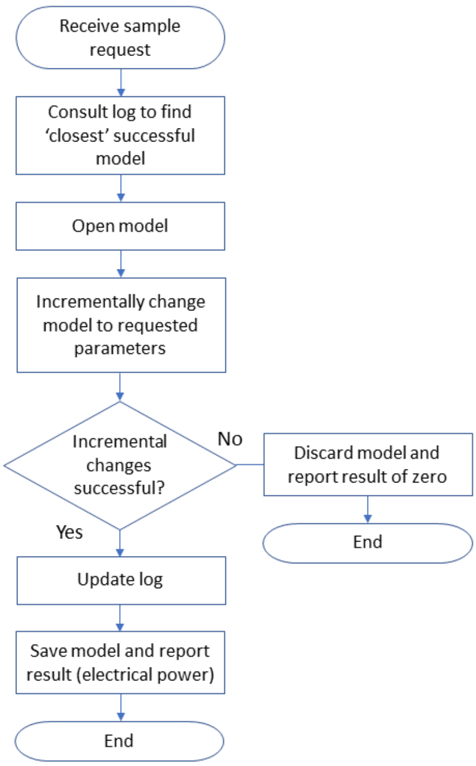

Figure 3. Flowchart describing the automated sampling script.

Development of an automated sampling script allowed various different approaches to optimisation to be trialled.

3.4 Global Optimisation (Design of Experiments Approach)

Firstly, the DOE approach to optimisation was attempted by performing an initial full factorial experiment. Each parameter was assigned 4 levels as a compromise between resolution and data acquisition speed. In the case of this study, with 5 parameters each set at 4 levels the initial experiment had 1024 sample points. The automated process to gather this data took 12 hours and only 30 of the sample points resulted in a successful run by DeltaEC. This corresponds to one evaluation of the model per 42 seconds. The methodology employed at this stage is shown in Figure 4.

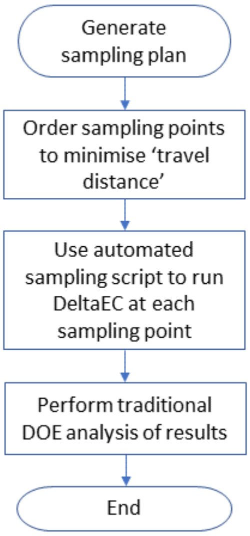

Figure 4. Flowchart describing the automated design of experiments approach.

Data analysis is complicated by the unsuccessful sample points. A value of 0 W output is assigned to these sample points, however other missing data representations could be used such as Not-a-Number (NaN). If these zero values are included in analysis, then any relationship is highly skewed. Whereas if the data is limited to successful sample points only, the sample becomes biased. The unsuccessful results can be included using missing-not-at-random (MNAR) statistical techniques [30], but the process is very involved and available conclusions are limited with a high level of uncertainty. The portion of the data that is MNAR makes this a worthless task. Smaller experiments could be designed using fractional factorial designs but the problem of a large proportion of unsuccessful sample points would remain.

In conclusion, global sampling using DOE techniques is not feasible for optimisation of DeltaEC models due to the large number of sample points required to resolve the small region of simulation convergence and the associated high run time. However, this experiment did serve to identify the region of interest where successful simulation is possible.

Consequently, global optimisation was also discarded as a feasible approach for this study. This is because any global approach will require sampling distributed across the whole sample space. With the current method of sampling, where every sample point has to be generated from a previous successful run via small incrementations, this is too time consuming. However, the approach taken in this pilot study does show that a global optimisation technique is possible given enough computational time.

3.5 Local Optimisation (Nelder-Mead Optimisation)

Secondly, a local optimisation was performed. In this case the mean pressure was varied manually before optimisation of the stub parameters was performed. This allows comparison of the performance of tuned engines at different mean pressures.

The Nelder-Mead scheme was chosen over other derivative-free, local optimisation schemes due to its ease of implementation using the SciPy module [31]. The particular implementation of the method is based on the paper by Gao and Han [32] and adapted to accept parameter bounds based on the paper by Luersen, et al. [33]. The implementation of a bounded search is critical as the dimensions of some components of the TAE are constrained. The implementation of the Nelder-Mead algorithm in relation to DeltaEC is shown in Figure 5.

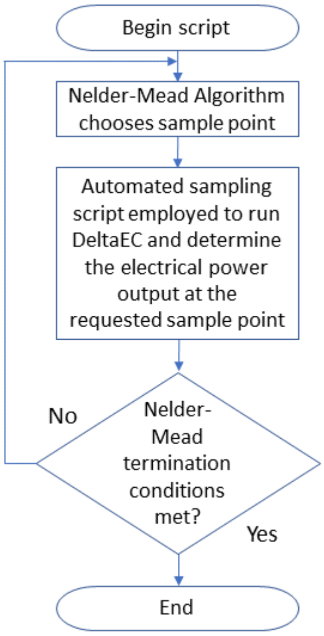

Figure 5. Flowchart showing the local optimisation process.

Non-reliance on gradient information is essential for DeltaEC where a large area of the input space will result in unsuccessful runs. Optimisation algorithms often estimate the gradient in the absence of an analytical gradient via finite difference methods or by monitoring elementary operations during the computation process [18]. However, gradient estimation in the region of discontinuities (such as the boundary between successful and unsuccessful DeltaEC runs) is not meaningful. The Nelder-Mead algorithm has been shown to be insensitive to small imprecisions or stochastic effects in the evaluated function [34], however this is unlikely to be significant for numerical simulation.

3.6 Main Study

A local optimisation using the Nelder-Mead algorithm was chosen as the final optimisation approach.

Initially, the TAE models with mean pressures of atmospheric, 2,3,4 and 5 bar were optimised. A further four pressures were investigated to determine the peak electrical output to a tolerance of ± 0.1 bar. All optimisations proceeded for a maximum of 200 samples with convergence defined as a change in less than 0.05 W between iterations. This condition was reached in 4 out of the 9 optimisations. However, reaching this convergence condition was not critical due to the heuristic nature of the search. It was judged that improvement after 200 iterations would be insignificant. The flat nature of the model near the optimum poses a problem for convergence as the sensitivity to convergence tolerance is high.

Figure 6 shows the typical progression of the optimisation algorithm. It is seen that the rate of improvement of the electrical output is slow beyond 100 iterations. Beyond this point only small improvements are made despite significant changes in the parameters.

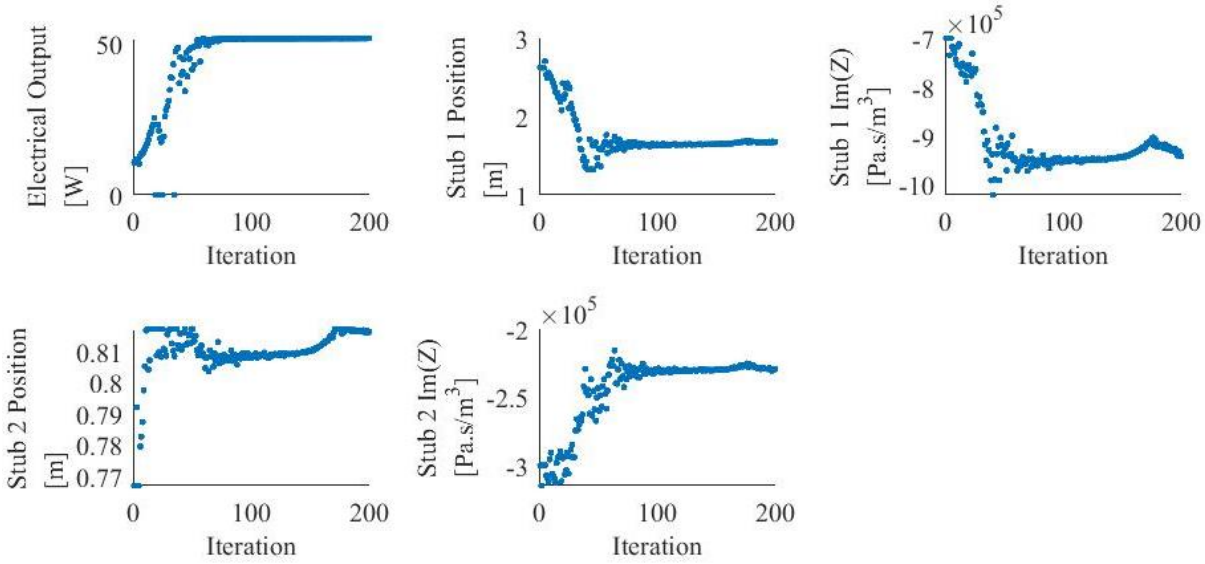

Figure 6. Progression of the Nelder-Mead optimisation algorithm for a mean pressure of 3 bar. Stub position is consistent with distance, x in Figure 2b.

Automation with the Nelder-Mead algorithm required a mean of 28 seconds per sample of the model. This is less than the DOE approach due to the shorter 'travel' required between sample points.

It was found that the choice of load resistor (load matching) was primarily dependant on mean pressure. As each optimisation process occurs at a constant pressure, only the final, optimised model is load matched using Brent's Method (a scalar optimisation algorithm) implemented in SciPy.

4. Discussion and Results

All proceeding discussion relates to the DeltaEC models after Nelder-Mead optimisation.

4.1 Stub Position and Length

The relationships between optimal stub parameters and mean pressure is shown in Figure 7. Note that each of the contour plots are formed by linear interpolation from 9 data points. The length of both stubs increases with pressure, whereas the positions of stubs do not show a trend with respect to pressure. This lack of trend can be explained by the starting parameter setting for each optimisation. The number of iterations required before significant improvement slows is partly determined by the proximity of the starting parameter settings to the optimum parameter settings. The large variation in stub parameters after this point was not accounted for when completing the optimisation and consequently the effect of initial parameter settings obscures any trend.

The effect of initial conditions could be negated by using the Globalised Restart Nelder Mead (GBNM) algorithm [35]. This enhancement involves repeatedly running the Nelder-Mead algorithm from randomly selected starting points. However, this method cannot easily be implemented in the case of DeltaEC as the limits of the sample space compatible with successful DeltaEC runs would need to be known in advance, in order to select feasible starting points.

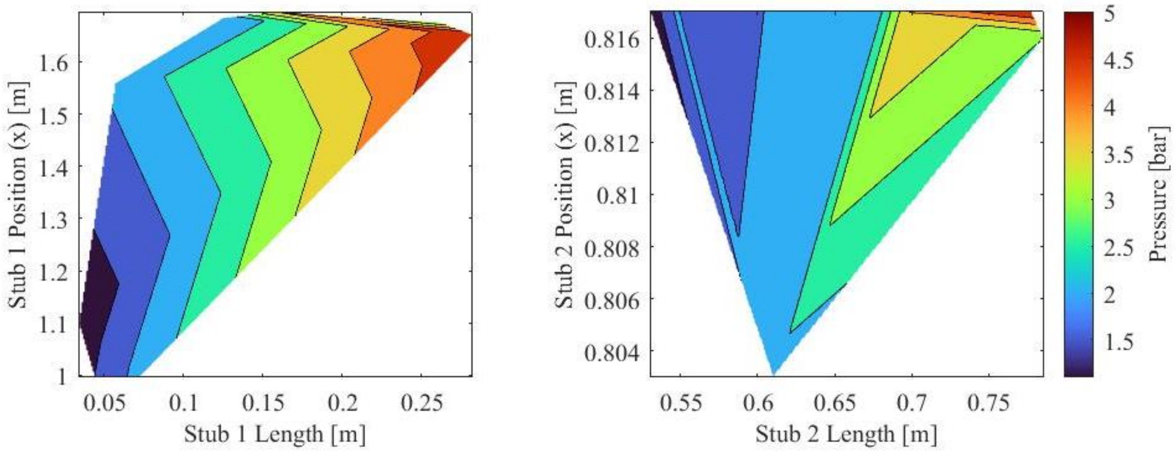

Figure 7. Contour plots for the optimal stub parameters with varying mean pressure.

4.2 Power Output

The relationship between pressure and electrical power output is shown in Figure 8a. Figure 8a also shows the acoustic power at the loudspeaker. Acoustic power continuously increases with mean pressure confirming theory (Equation 1). However, electrical power output reaches a maximum of 59.63 W at 2.2 bar. This power output is an increase of 16.14 W compared to the tuned engine at 1 atmosphere mean pressure.

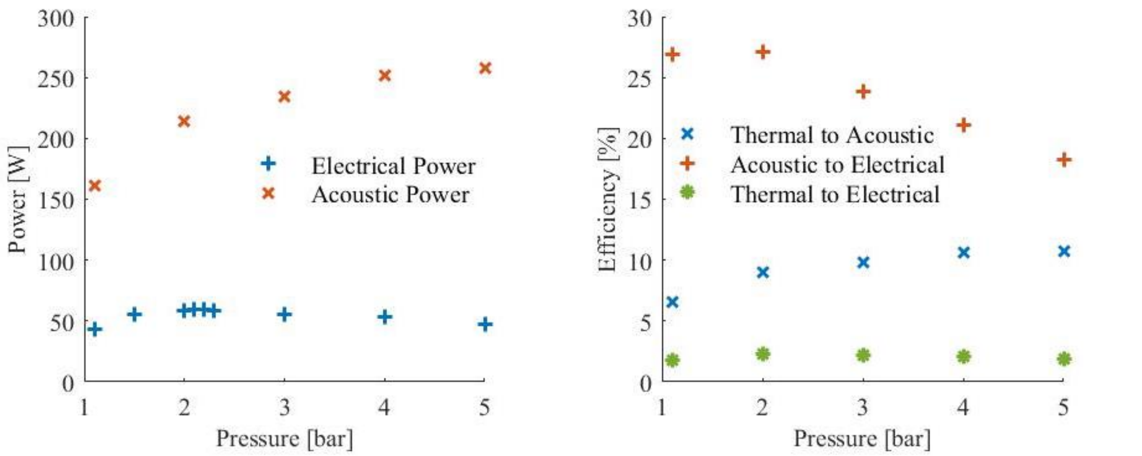

Figure 8. a) Acoustic and electrical power developed by the TAE with varying mean pressure. b) Efficiencies of the TAE with varying mean pressure

A significant (90%) improvement has been made in theoretical power output. However, it cannot be explicitly proven that the DeltaEC model has been fully optimised within the parameter boundaries due to the nature of the algorithm used. Future work is required to experimentally validate these results. The experimental results are likely to produce lower powers than DeltaEC due to the absence of effects in the numerical model such as mass streaming and thermal radiation [26]. Kisha, et al. [27] reported a decrease in power from the numerical model to experiment of 27-32% and Riley [11] reported decreases of 30%.

Figure 8b shows the efficiency of various power conversions in the engine. Thermal to acoustic efficiency increases with pressure whereas acoustic to electrical efficiency has a peak in the region of 2 bar. This corresponds to the peak in thermal to electric efficiency of 2.385% at 2.2

bar. This is similar to numerical simulations of comparable TAEs, achieving thermal to electric efficiency of 2.4% [29] and 2.5% [16].

The eventual decrease in acoustic to electrical efficiency indicates that the power extracted by the loudspeaker is not proportional to the acoustic power at the loudspeaker. The decrease in acoustic power extracted can be attributed to at least two factors:

1. *Decreasing volumetric velocity*

The acoustic power removed from the TAE is a function of acoustic parameters either side of the loudspeaker. This is described by Equation 3 [36]:

$$P = \frac{1}{2}|U_1|\{p_1 cos(\theta_a) - p_2 cos(\theta_b)\} \tag{3}$$

U is volumetric velocity, p is pressure and θ is phase angle. The subscripts 1 and 2 refer to the position adjacent to the loudspeaker on the side of high and low acoustic power, respectively. θ_a is the phase angle between p_1 and U_1, θ_b is the phase angle between p_2 and U_1. Plotting both components of Equation 3 (Figure 9) shows that a decreasing volumetric velocity is responsible for decreasing power despite an increasing pressure difference.

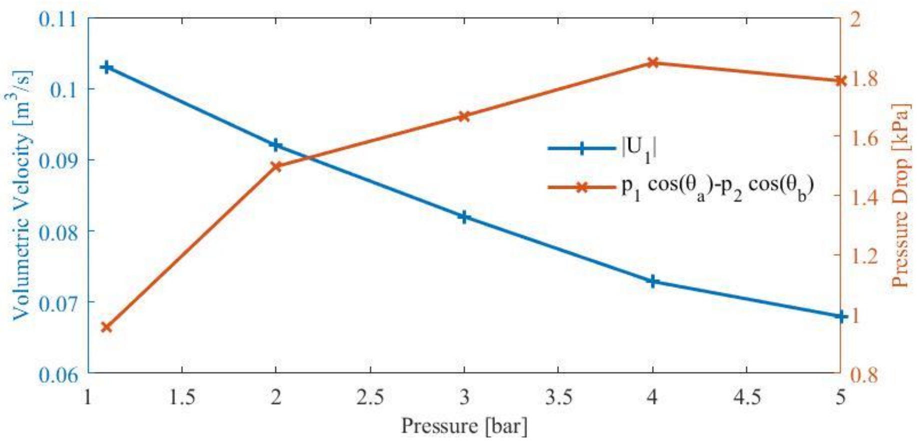

Figure 9. Volumetric velocity and pressure drop across loudspeaker.

The decrease in volumetric velocity is explained using the following one-dimensional, first order differential equation derived from decoupling the second order 'wave equation' [8]. The equation presented omits viscous or thermal relaxation losses.

$$dU = -\left(\frac{i\omega A}{\gamma p_m} p\right) dx \tag{4}$$

U is volumetric velocity, p is pressure, ω is frequency, A is cross sectional area, x is length and γ is the ratio of specific heats. The subscript m refers to mean. Equation 4 shows that the change in volumetric velocity over a length, dx decreases with increasing mean pressure.

2. *Decreasing operating frequency*

One of the conditions for maximising the efficiency of the loudspeaker is to operate it at the frequency corresponding to its mechanical resonance [12]. The resonance of the loudspeaker is 77.19 Hz, whereas the operating frequency of the TAE decreases from 75.21 Hz at 1 bar to 71.52 Hz at 5 bar. Therefore, the contribution of resonance to efficiency decreases with increasing pressure. Riley [11] relates operating frequency as a function of feedback pipe length and parasitic volume. Feedback pipe length is kept constant and therefore it is postured that increasing stub length is partly responsible for the decrease in frequency. The length of the feedback pipe may be optimised to raise the frequency closer to 77.19 Hz, however this will have competing effects elsewhere.

4.3 Acoustic Field

Table 2 details the positions of selected components with major influence on the acoustic field. The position (x) is measured from the ambient temperature side of regenerator 2 as shown in Figure 2b.

Key component	Label in Figures 7 to 11	Position (x [m])
Regenerator 2	a	0.038
Loudspeaker	b	0.267
Stub 2	c	0.803-0.817
Regenerator 1	d	0.845
Stub 1	e	1.100 - 1.696
Feedback Loop	n/a	0.924 - 4.124

Table 2. Positions of key components in the TAE. The position (x) is consistent with Figure 2b.

Select acoustic fields of the tuned engine at three representative pressures are presented (Figures 10 to 14) for the purpose of providing context to the trends in acoustic and electrical power output with changing pressure. The vertical lines correspond to the position or range of positions where a component is situated, as described in Table 2.

The implication of changes in pressure, volumetric velocity and phase difference on acoustic power can be explained using Equation 5, which describes time-averaged acoustic power produced in a length, dx, of channel [12]. This equation describes the acoustic power gradient along x, in terms of pressure, p; volumetric velocity, U; phase difference between p and U, φ; specific viscous resistance, r_v; specific thermal resistance, r_k; and specific gain, g.

$$\frac{d\dot{E}}{dx} = -\frac{r_v}{2}|U|^2 - \frac{1}{2r_k}|p|^2 + \frac{1}{2}Re[gpUcos(\varphi)] \qquad (5)$$

Acoustic power (Figure 10) increases at higher mean pressures in accordance with Equation 1. The regenerators (a,d) augment acoustic power and the loudspeaker (b) diminishes it. The stubs (c,e) have little effect on acoustic power. Acoustic power decreases between components because of viscous losses and thermal relaxation (terms 1 and 2 of Equation 5). This can be seen in the feedback loop ($x = 0.924$ to 4.124) as a decreasing gradient. The rate of acoustic power loss in the feedback loop is higher at 1 bar (4.57 W/m) than at 5 bar (2.80 W/m). This indicates that decreasing volumetric velocity magnitude (Figure 12) is the dominant effect over increased pressure magnitude (Figure 11) contributing to power loss (Equation 5) in this area of the TAE.

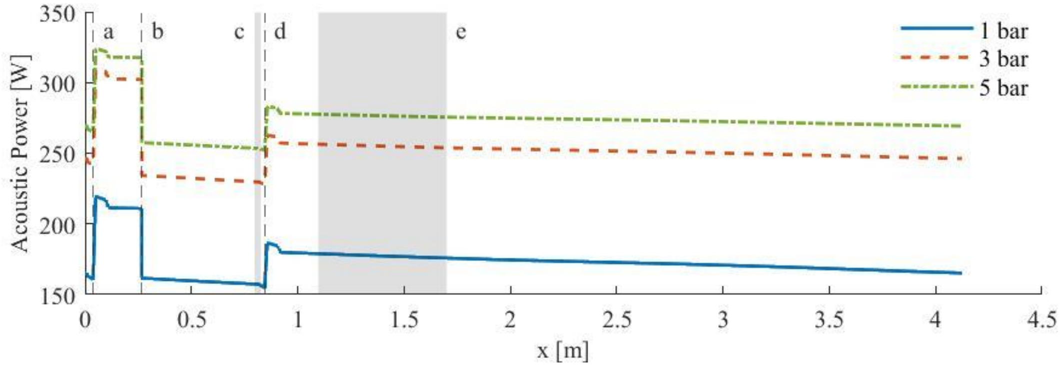

Figure 10. Variation of the acoustic power with position in the TAE for selected mean pressures.

In Figure 11, pressure amplitude increases with mean pressure as expected. Pressure amplitude drops at both regenerators (a,d) as a result of viscous losses. The pressure drop across the loudspeaker (b) indicates the acoustic power removed. The stubs (c,e) have little effect on the local pressure magnitude.

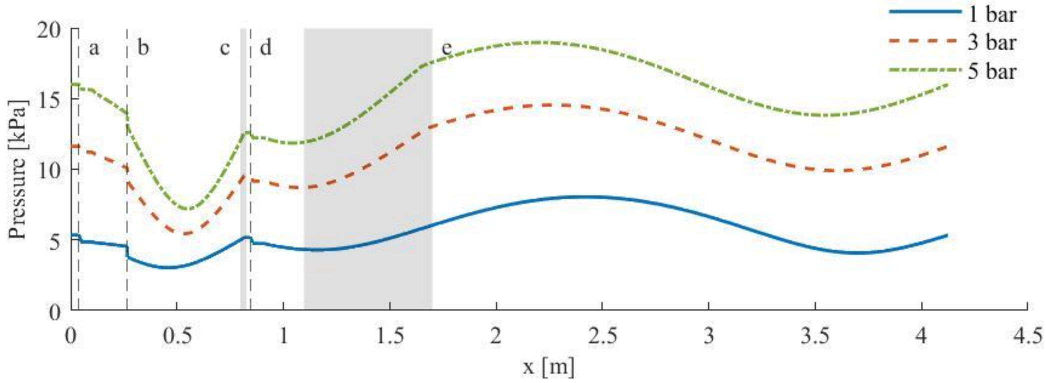

Figure 11. Variation of pressure amplitude with position in the TAE for selected mean pressures

The pressure standing-wave ratio (PSWR) shows minor variation with changing mean pressure. The median value is 2.655 across all mean pressures with a standard deviation of 0.0263. This indicates a significant standing wave in the feedback loop resulting in a decrease in efficiency. A PSWR of less than 1.8 is considered good for this type of TAE [11].

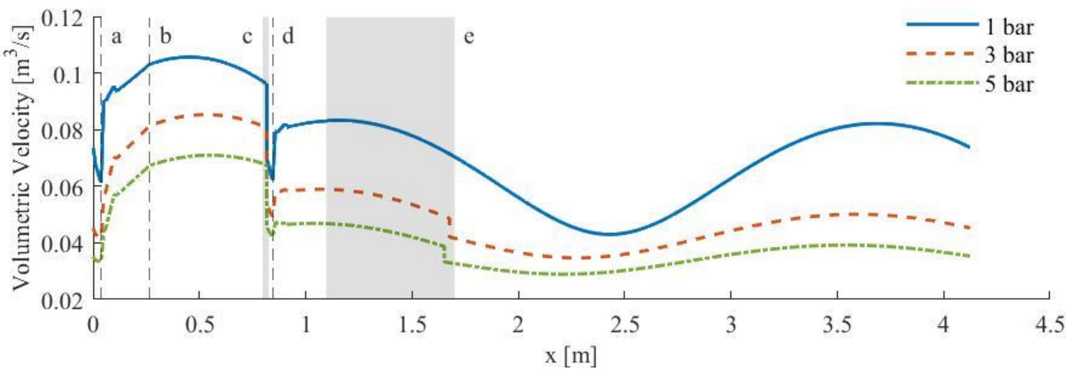

Figure 12. Variation of volumetric velocity magnitude with position in the TAE for selected mean pressures.

In Figure 12, volumetric velocity shows a decreasing trend with increased mean pressure. This results in efficiency increases within the TAE as viscous losses are reduced. However, it contributes to a decreasing electrical power output as described in Section 4.1. The position of the loudspeaker (b) is a compromise in maximising pressure amplitude (decreasing x) and maximising velocity amplitude (increasing x). A sharp increase in velocity occurs in the region of the two regenerators (a,d) as the flow accelerates due to the heat addition and resulting expansion. Both stubs (c,e) cause a decrease in volumetric velocity. The drop at stub 2 (c) results in an increase in efficiency as viscous losses in the regenerator are reduced as a result of the decreased entry velocity. Stub 1 (e) acts to adjust the position of the velocity nodes such that velocity is low entering regenerator 2 (a).

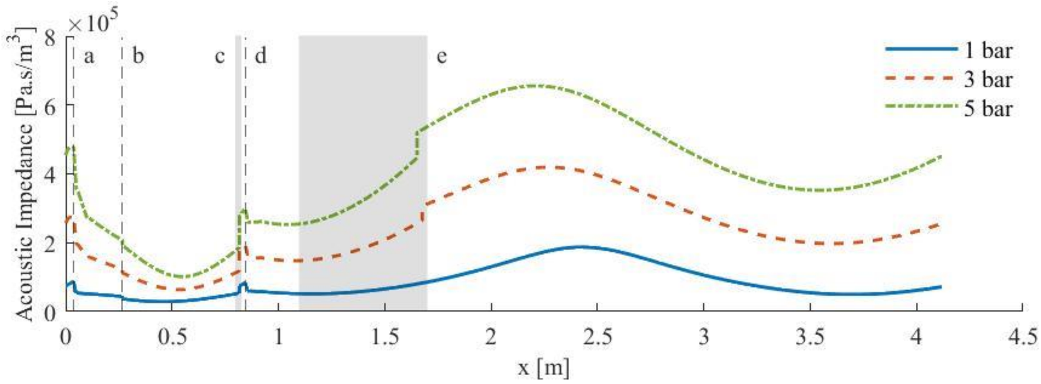

Figure 13. Variation of acoustic impedance magnitude with position in the TAE for selected mean pressures.

In Figure 13, acoustic impedance shows a trend of increasing with increasing mean pressure. This is a desirable trait at the regenerators as an increase in impedance within the regenerators reduces viscous losses [12]. The stubs (c,e) both increase acoustic impedance as a result of decreasing volumetric velocity and negligible pressure change. The magnitude of this impedance change increases with a higher mean pressure. The regenerators (a,d) decrease impedance due to increased velocity and the loudspeaker (b) decreases acoustic impedance due to the decreased pressure.

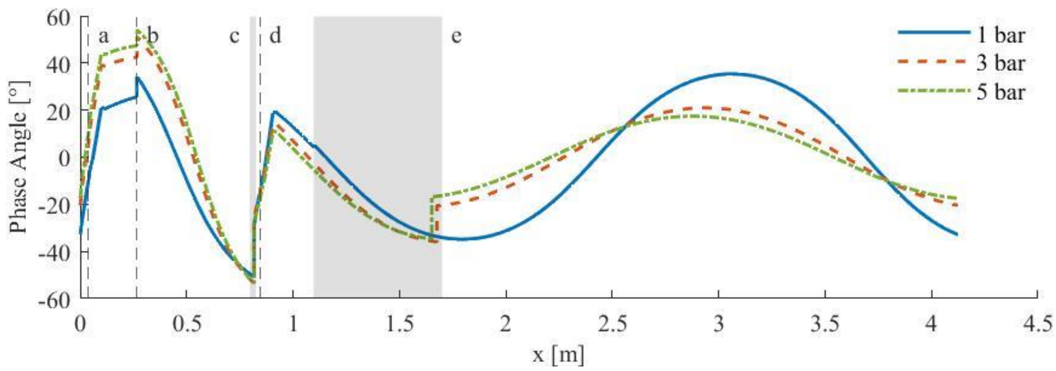

Figure 14. Variation of the phase difference between pressure and volumetric velocity with position in the TAE for selected mean pressures.

Figure 14 shows the action of both stubs to increase regenerator efficiency. Both stubs act to move the phase difference at the succeeding regenerator closer to zero, thereby maximising the acoustic power gain (term 3, Equation 5). However, a trend in this action is not discernible with changing mean pressure. A higher pressure results in greater phase difference at the loudspeaker (b) but decreased phase difference in the feedback loop, indicating a better travelling wave condition.

Onset temperature difference for both regenerators decreases with increasing pressure. The values for regenerator 1 decreased from 120°C to 67°C, whereas the values for regenerator 2 decreased from 184°C to 121°C. The onset temperature is a measure of acoustic matching between components, with a lower temperature indicating better matching [11].

5. Future Research

The local search employed in this paper is limited by 1) the inability to quantify optimality of the local solution, 2) the limited information on main and interaction parameter effects, and 3) the lack of guarantee of a global solution.

Surrogate modelling is a type of supervised machine learning [37] that aims to create a numerical model to approximate a simulation output. This numerical model can then be employed to perform global optimisation as well as sensitivity and risk analysis. It is identified as an effective approach to working with DeltaEC to further understand parameter interactions and optimise if necessary. The process starts with an initial, global sample (training sample) based on DOE sampling schemes. In this case performing a global DOE is more acceptable due to the greater reward of a surrogate model and the significantly reduced number of required sample points – as the initial goal is not to resolve the optimum. An iterative approach is then used to approximate the data with a model and intelligently identify more sample points in order to improve the model (active learning). Optimisation by surrogate modelling is identified as being highly efficient (least number of function evaluations, most information recovered) however the implementation is a subject for future work. A particular nuance of applying this approach to DeltaEC is accepting the results of failed simulations. This problem can be addressed by the imputation approach detailed by Forrester, et al. [37].

6. Conclusions

This numerical study shows that increasing the mean pressure in a twin-core, asymmetrically heated thermoacoustic engine increases electrical power output. The maximum electrical output is 59.63 W achieved at 2.2 bar mean pressure. However, these simulation results need to be verified experimentally. Cost analysis is required to determine if the hardware and manufacturing costs required for a 2.2 bar mean pressure TAE are acceptable. The peak in electrical power output is a result of a decrease in both volumetric velocity and operating frequency at increased mean pressure. The development of automation techniques for DeltaEC enables the use of algorithmic optimisation allowing for quick determination of optimal parameters considering system level parameter interactions. This is especially applicable for tuning the acoustic field using side branched volumes (stubs). This type of algorithmic optimisation could be applied to any continuous design parameter(s) of a TAE. The automated approach developed for this study allows fast data gathering from DeltaEC models and may be adapted for other studies not necessarily involving optimisation. Optimisation by surrogate modelling is one approach recommended for future studies.

Acknowledgements

The author would like to thank Greg Swift for help using Python to automate DeltaEC.

References

[1] United-Nations, "Sustainable Development Goals," 2018. [Online]. Available: https://unstats.un.org/sdgs/report/2018/goal-07
[2] WHO. "Global health observatory data repository." WHO. (accessed 2020).
[3] K. K. Lee *et al.*, "Adverse health effects associated with household air pollution: a systematic review, meta-analysis, and burden estimation study," *The Lancet Global Health,* Article vol. 8, no. 11, pp. e1427-e1434, 2020, doi: 10.1016/S2214-109X(20)30343-0.

[4] P. H. Riley, "Affordability for sustainable energy development products," *Applied Energy,* Article vol. 132, pp. 308-316, 2014, doi: 10.1016/j.apenergy.2014.06.050.

[5] B. M. Chen, P. H. Riley, Y. A. Abakr, K. Pullen, D. B. Hann, and C. M. Johnson, "Design and development of a low-cost, electricity-generating cooking Score-Stove™," *Proceedings of the Institution of Mechanical Engineers, Part A: Journal of Power and Energy,* Article vol. 227, no. 7, pp. 803-813, 2013, doi: 10.1177/0957650913498733.

[6] T. Biwa, D. Hasegawa, and T. Yazaki, "Low temperature differential thermoacoustic Stirling engine," *Applied Physics Letters,* Article vol. 97, no. 3, 2010, Art no. 034102, doi: 10.1063/1.3464554.

[7] K. De Blok, "Multi-stage traveling wave thermoacoustics in practice," in *19th International Congress on Sound and Vibration 2012, ICSV 2012*, 2012, vol. 2, pp. 1573-1580.

[8] N. Rott, "Damped and thermally driven acoustic oscillations in wide and narrow tubes," *Zeitschrift für angewandte Mathematik und Physik ZAMP,* Article vol. 20, no. 2, pp. 230-243, 1969, doi: 10.1007/BF01595562.

[9] A. Bodrov, M. Zhang, R. Shuttleworth, and M. F. Iacchetti, "Sensorless Control of a Linear Generator for Energy Harvesting Applications," in *2019 12th International Symposium on Linear Drives for Industry Applications, LDIA 2019*, 2019, doi: 10.1109/LDIA.2019.8770976.

[10] M. A. G. Timmer and T. H. Van Der Meer, "Optimizing bidirectional impulse turbines for thermoacoustic engines," *Journal of the Acoustical Society of America,* Article vol. 147, no. 4, pp. 2348-2356, 2020, doi: 10.1121/10.0001067.

[11] P. H. Riley, "Designing a low-cost electricity-generating cooking stove for high-volume implementaion," 2014.

[12] G. W. Swift, *Thermoacoustics: A Unifying perspective for some engines and refrigerators* (Thermoacoustics: A Unifying Perspective for Some Engines and Refrigerators). 2002.

[13] J. R. Olson and G. W. Swift, "Similitude in Thermoacoustics," *Journal of the Acoustical Society of America,* Article vol. 95, no. 3, pp. 1405-1412, 1994, doi: 10.1121/1.408581.

[14] Z. Wu, G. Yu, L. Zhang, W. Dai, and E. Luo, "Development of a 3kW double-acting thermoacoustic Stirling electric generator," *Applied Energy,* Article vol. 136, pp. 866-872, 2014, doi: 10.1016/j.apenergy.2014.04.105.

[15] A. Al-Kayiem and Z. Yu, "Using a side-branched volume to tune the acoustic field in a looped-tube travelling-wave thermoacoustic engine with a RC load," *Energy Convers. Manage.,* Article vol. 150, pp. 814-821, 2017, doi: 10.1016/j.enconman.2017.03.019.

[16] K. O. A. Abdoulla-Latiwish and A. J. Jaworski, "Two-stage travelling-wave thermoacoustic electricity generator for rural areas of developing countries," *Applied Acoustics,* Article vol. 151, pp. 87-98, 2019, doi: 10.1016/j.apacoust.2019.03.010.

[17] Z. Yu, A. J. Jaworski, and S. Backhaus, "A low-cost electricity generator for rural areas using a travelling-wave looped-tube thermoacoustic engine," *Proceedings of the Institution of Mechanical Engineers, Part A: Journal of Power and Energy,* Article vol. 224, no. 6, pp. 787-795, 2010, doi: 10.1243/09576509JPE864.

[18] A. Gosavi, "Simulation-Based Optimization: An Overview," in *Simulation-Based Optimization: Parametric Optimization Techniques and Reinforcement Learning*, A. Gosavi Ed. Boston, MA: Springer US, 2015, pp. 29-35.

[19] J. Antony and J. Antony, *Design of Experiments for Engineers and Scientists*. Jordan Hill, UNITED KINGDOM: Elsevier, 2003.

[20] J. Nelder and R. Mead, "A Simplex Method for Function Minimization," *Comput. J.,* vol. 7, pp. 308-313, 1965.

[21] H. Ghiasi, D. Pasini, and L. Lessard, "Constrained globalized Nelder-Mead method for simultaneous structural and manufacturing optimization of a composite bracket," *Journal of Composite Materials,* Article vol. 42, no. 7, pp. 717-736, 2008, doi: 10.1177/0021998307088592.

[22] W. F. Sacco, H. A. Filho, N. Henderson, and C. R. E. de Oliveira, "A Metropolis algorithm combined with Nelder-Mead Simplex applied to nuclear reactor core design," *Annals of Nuclear Energy,* Article vol. 35, no. 5, pp. 861-867, 2008, doi: 10.1016/j.anucene.2007.09.006.

[23] Z. Romani, A. Draoui, and F. Allard, "Metamodeling the heating and cooling energy needs and simultaneous building envelope optimization for low energy building design in Morocco," *Energy and Buildings,* Article vol. 102, pp. 139-148, 2015, doi: 10.1016/j.enbuild.2015.04.014.

[24] A. Gosavi, "Parametric Optimization: Stochastic Gradients and Adaptive Search," in *Simulation-Based Optimization: Parametric Optimization Techniques and Reinforcement Learning*, A. Gosavi Ed. Boston, MA: Springer US, 2015, pp. 71-122.

[25] J. C. Lagarias, J. A. Reeds, M. H. Wright, and P. E. Wright, "Convergence properties of the Nelder-Mead simplex method in low dimensions," *SIAM Journal on Optimization,* Article vol. 9, no. 1, pp. 112-147, 1998, doi: 10.1137/S1052623496303470.

[26] J. Clark, W. Ward, and G. Swift, "Design environment for low-amplitude thermoacoustic energy conversion (DeltaEC)," *Journal of the Acoustical Society of America,* vol. 122, pp. 3014-3014, 2007.

[27] W. Kisha, P. Riley, J. McKechnie, and D. Hann, "Asymmetrically heated multi-stage travelling-wave thermoacoustic electricity generator," *Energy,* vol. 235, p. 121312, 2021/11/15/ 2021, doi: https://doi.org/10.1016/j.energy.2021.121312.

[28] P. H. Riley, "SoFo Executive Meeting," ed, 2012.

[29] Z. Yu, A. J. Jaworski, and S. Backhaus, "Travelling-wave thermoacoustic electricity generator using an ultra-compliant alternator for utilization of low-grade thermal energy," *Applied Energy,* Article vol. 99, pp. 135-145, 2012, doi: 10.1016/j.apenergy.2012.04.046.

[30] J. L. Schafer and J. W. Graham, "Missing data: Our view of the state of the art," *Psychological Methods,* Article vol. 7, no. 2, pp. 147-177, 2002, doi: 10.1037/1082-989X.7.2.147.

[31] K. J. Millman and M. Aivazis, "Python for Scientists and Engineers," *Computing in Science & Engineering,* vol. 13, no. 2, pp. 9-12, 2011, doi: 10.1109/MCSE.2011.36.

[32] F. Gao and L. Han, "Implementing the Nelder-Mead simplex algorithm with adaptive parameters," *Computational Optimization and Applications,* Article vol. 51, no. 1, pp. 259-277, 2012, doi: 10.1007/s10589-010-9329-3.

[33] M. A. Luersen, R. Le Riche, and F. Guyon, "A constrained, globalized, and bounded Nelder-Mead method for engineering optimization," *Structural and Multidisciplinary Optimization,* Article vol. 27, no. 1-2, pp. 43-54, 2004, doi: 10.1007/s00158-003-0320-9.

[34] R. R. Barton and J. S. Ivey, "Nelder-Mead Simplex Modifications for Simulation Optimization," *Management Science,* vol. 42, no. 7, pp. 954-973, 1996.

[35] M. A. Luersen and R. Le Riche, "Globalized Nelder–Mead method for engineering optimization," *Computers & Structures,* vol. 82, no. 23, pp. 2251-2260, 2004/09/01/ 2004.

[36] Z. Yu, P. Saechan, and A. J. Jaworski, "A method of characterising performance of audio loudspeakers for linear alternator applications in low-cost thermoacoustic electricity generators," *Applied Acoustics,* Article vol. 72, no. 5, pp. 260-267, 2011, doi: 10.1016/j.apacoust.2010.11.011.

[37] A. I. J. Forrester, A. Sóbester, and A. Keane, *Engineering Design via Surrogate Modelling*. Wiley, 2008.